Research Square

Preprints are preliminary reports that have not undergone peer review.
They should not be considered conclusive, used to inform clinical practice,
or referenced by the media as validated information.

Grasp Dexterity Index: Manipulability of Objects Grasped by Multi-fingered Robotic Hands

S. Barat
Indian Institute of Technology Gandhinagar
Vatsal Ketankumar Joshi
Indian Institute of Technology Gandhinagar
Debojit Das
debojit.das@iitgn.ac.in

Indian Institute of Technology Gandhinagar
Harish J. Palanthandalam-Madapusi
Indian Institute of Technology Gandhinagar

Research Article

Keywords: grasp dexterity index, grasp manipulability, multi-fingered robotic hands, in-hand manipulation, redundancy optimization, human grasping

Posted Date: May 14th, 2026

DOI: https://doi.org/10.21203/rs.3.rs-9620791/v1

License: This work is licensed under a Creative Commons Attribution 4.0 International License.
Read Full License

Additional Declarations: No competing interests reported.

Grasp Dexterity Index: Manipulability of Objects Grasped by Multi-fingered Robotic Hands

S. Barat[1†], Vatsal Ketankumar Joshi[1†], Debojit Das[1*], Harish J. Palanthandalam-Madapusi[1]

[1]IITGN Robotics Laboratory, Department of Mechanical Engineering, Indian Institute of Technology Gandhinagar, Gandhinagar, Gujarat, 382355, India.

*Corresponding author(s). E-mail(s): debojit.das@iitgn.ac.in;
Contributing authors: barats@iitgn.ac.in; vatsaljoshi00@gmail.com; harish@iitgn.ac.in;
†These authors contributed equally to this work.

Abstract

In-hand manipulation of a grasped object or force production using a grasped object with a multi-fingered hand requires an understanding of the relationship between grasp configurations and object manipulability. Object manipulability is not only a function of the planned grasp, including the number of fingers used for grasping and the contact points on the object, but is also a function of the in-hand positioning of the held object and specific finger configurations within the range of infinitely many redundant configurations. While there is a significant body of work on grasp planning and manipulability for serial-chain manipulators, there is a need for a simple and practical metric that combines all factors important for determining the manipulability of a grasped object, particularly for a multi-fingered, multi-degree-of-freedom hand. In this work, we develop the Grasp Dexterity Index (GDI) as a combined metric that takes advantage of existing manipulability metrics, and we analyse the utility of this metric through simulation test cases, including cases that vary in-hand position and internal motions, and through a pilot-scale human study with six different day-to-day objects. This research provides an important step toward better evaluation of robot manipulation tasks with multi-fingered, multi-degree-of-freedom hands.

Keywords: grasp dexterity index, grasp manipulability, multi-fingered robotic hands, in-hand manipulation, redundancy optimization, human grasping

1 Introduction

With the rapid development of multi-finger, multi-degrees-of-freedom (multi DOF) robot hands (graspers) along with the increased complexity of robot manipulation and in-hand manipulation tasks, both grasp planning and grasp evaluation have become important areas. Given the infinitely many configurations in which an object can be held, grasp planning (planning how many fingers to use for grasping and the contact points on the object) is an important challenge and has received much attention [1]. In addition to planning contact points, there are two other factors that affect the quality of grasp and the ability to manipulate the object within the grasp. The first factor is the in-hand object positioning (that is, the relative position and orientation of the grasped object relative to the palm of the hand), and the second factor is the finger poses for the same in-hand object positioning (due to redundant degrees of freedom in each finger). While a substantial body of research exists on grasp planning, including various metrics and learning-based algorithms [1], relatively fewer studies focus on evaluating the quality of different in-hand positions and varying finger poses for the same contact points. Notable exceptions include [2], where the authors explored grasp synthesis and manipulability measures, addressing some of these critical aspects. Since in multi-finger, multi-DOF robot hands, infinitely many in-hand positioning configurations are possible for the same grasp contact points, and the same in-hand position (using internal motions in the fingers), simple, practical, and generalisable metrics that capture all three aspects of grasp configuration are needed. While the other factors, namely in-hand positioning and redundancy in finger pose configuration, are not as

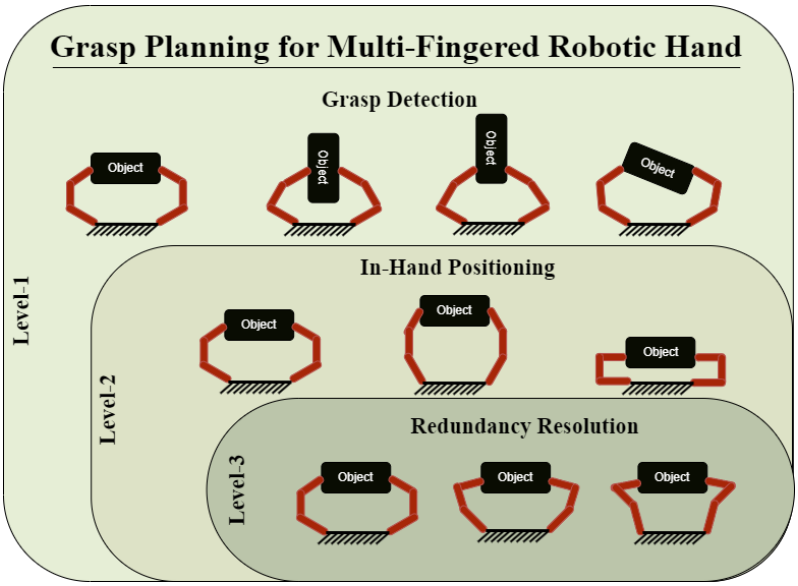


Fig. 1: Hierarchical Framework for Grasp Planning in Multi-Fingered Robotic Hands: Level 1 focuses on grasp detection, Level 2 emphasizes in-hand positioning, and Level 3 addresses redundancy resolution for optimizing grasp quality.

important when performing pick-and-place or simple grasping tasks, they become particularly important when performing in-hand manipulation or force-production tasks with the held object after picking it up. For example, when the task is to pick up a pen and then press it against paper to write, even for the same contact points on the pen, different grasp poses provide different abilities to manipulate the object and produce forces. Likewise, when one grasps and rotates a knob, different grasp poses for the same contact points yield different manipulation abilities. In all such cases, simply grasping the object stably is not sufficient; it is useful to optimise the grasp pose to perform additional motion or force-production tasks.

Among related works, there is a significant body of work on metric and evaluation for grasp planning. Significant research has also been conducted by employing grasp mechanics theory [3]. [4] develops a precise and efficient method to improve grasp planning, significantly enhancing the grasping of long and thin objects. A practical approach was adopted in [5] for parallel jaw gripper systems to perform antipodal grasping. Furthermore, [6] reviews several grasp quality metrics based on the first-principles model of robot grasping, considering both grasp configuration and hand configuration through serial or parallel approaches. Other related works include those that use manipulability metrics for performing dual-arm and free-floating space robot collaborative manipulation [7], [8]. Kinematic and force analyses have been performed for underactuated grippers with compliant contact and actuation [9]. [10] introduces a Fingertip Manipulability (FtM) Metric to evaluate finger performance for tendon-driven robotic hands through real-time planning and performance monitoring. A manipulability measure is devised in [11] to select grasp poses with rolling contacts for multi-fingered robots. There are also a rapidly growing body of work on approaches that use optimization, vision, and deep learning methods for approaches for grasp planning and evaluation [12–19]. These methods are promising and have delivered successful results; however, they require robust datasets to perform grasping tasks for a wide range of objects.

Given that humans excel in dexterous manipulation, extensive focus has been placed on comparing and drawing inspiration from human grasp approaches. [20] demonstrates the comparison of anthropomorphic motion capability among different types of artificial robotic hands with a human hand using a Gaussian process latent variable model (GP-LVM). A more human-centered approach was adopted in [21], which uses human grasping experience and shape affordance to grasp familiar objects. To minimize grasp effort, a physiologically based method was developed to grasp objects using human hand precision grip posture [22].

As apparent from the discussions thus far, most of the existing works focus on evaluating grasp planning strategies and formulating metrics to quantify grasp quality, and there has been limited exploration of optimizing or in-hand positioning or finger poses once the object is grasped. A significant area of need is thus a simple metric helping evaluate the combined effect of grasp configuration, in-hand positioning, and finger poses, for a well-rounded quantification of grasp quality.

Our work focuses on designing a metric inspired by [7] and [6], which quantifies the combined effects of multiple factors, emphasizing in-hand manipulations and finger

poses. We introduce this metric as the Grasp Dexterity Index (GDI). The mathematical formulation of grasp theory and grasp manipulability is detailed in Section 2. Section 3 explores various existing grasp indexes and their inter-relationships. In Sections 4, 5, and 6, we present simulation-based case studies to analyze grasp manipulability metrics in depth, discuss their limitations, and demonstrate the formulation and evaluation of the GDI. Section 7 examines the GDI in practical robot grasping scenarios and bi-manual manipulation tasks. Furthermore, Section 8 discusses a pilot study involving human subjects performing six different object grasping tasks—using both pinch and tripod grasps—to showcase the utility of the GDI.

2 Modeling and Methodology

Each finger and the object are assumed to have a single contact point (C_i), with no slip between their surfaces [3]. At contact point C_i, let s_i and t_i represent the tangential unit vectors, and n_i the unit vector along the common normal oriented towards the object's center of gravity. f_t^i and f_s^i denote tangential contact forces and f_n^i denotes normal contact force exerted on the object surface by the i^{th} finger, respectively. Consider F_b as the object frame with its origin at the object's center of gravity, and F_w as the fixed world frame. Let b_i and x_i represent the position vector to the i^{th} contact point from F_b and F_w respectively, with d being the Euclidean distance between the origins of F_b and F_w. $R(\theta)$ denotes the rotation matrix for the object relative to F_w. At an object position and orientation q, the block column $G_i(q) \in \mathbb{R}^{6\times3}$ of the Grasp Matrix is defined as follows:

$$G_i(q) = \begin{bmatrix} s_i & t_i & n_i \\ R(\theta)b_i \times s_i & R(\theta)b_i \times t_i & R(\theta)b_i \times n_i \end{bmatrix}. \tag{1}$$

The full grasp matrix $G(q) \in \mathbb{R}^{6\times3k}$ captures the relationship for a gripper with k fingers and k contact points as

$$G(q) = \begin{bmatrix} G_1(q) & G_2(q) & \cdots & G_k(q) \end{bmatrix}. \tag{2}$$

The second component necessary for evaluating the manipulability index is the hand Jacobian $J_H \in \mathbb{R}^{kp\times N}$, defined as

$$J_H(\phi, q) = \begin{bmatrix} W_1^T R_{PK_1} J_1(\phi_1) & 0 & \cdots & 0 \\ \vdots & & \ddots & \vdots \\ 0 & 0 & \cdots & W_k^T R_{PK_k} J_k(\phi_k) \end{bmatrix}. \tag{3}$$

where N signifies the total number of joints. In this context, W_i denotes the contact frame basis of the i^{th} contact point in F_w, R_{PK_i} stands for the rotation matrix of the finger base frame relative to the palm frame, J_i represents the Jacobian of the i^{th} finger and ϕ represents joint states of the robot.

2.1 Mathematical Formulation

A quantitative measure of object grasp manipulability is crucial for precision grasping. To develop this index, we utilize the contact compatibility constraint equation in grasp kinematics $J_H(\phi, q)\dot{\phi} = G^T(q)\dot{q}$, and therefore

$$\dot{\phi} = J_H^{\dagger} G^T(q)\dot{q}. \tag{4}$$

Bounding the input norm of finger joint velocities as

$$\dot{\phi}^T \dot{\phi} \leq 1, \tag{5}$$

and substituting Eq. (4) into Eq. (5) gives us the equation for grasp manipulability ellipsoid

$$\dot{q}^T (G J^{\dagger T} J^{\dagger} G^T)\dot{q} \leq 1. \tag{6}$$

With $A \triangleq G^{\dagger T} J_H$, the above equation is then rewritten as

$$\dot{q}^T (A A^T)^{\dagger} \dot{q} \leq 1. \tag{7}$$

3 Investigating Various Grasp Indices

Manipulability indices have received significant attention in the study of serial chain manipulators [23]. Our aim is to re-purpose and utilise these indices in a grasping situation to develop an index quantifying grasp manipulability. We first examine several candidate metrics by using A from Eq. (7) and re-purposing the most common indices utilised in serial chain manipulators as illustrated in Table 1.

Table 1: Candidate grasp manipulability indices considered in this work.

Index	**Mathematical formulation**
Manipulability Index (MI)	$\sqrt{\det\left(AA^T\right)}$
Condition Number (CN)	$\frac{\sigma_{\max}\left(AA^T\right)}{\sigma_{\min}\left(AA^T\right)}$
Local Condition Index (LCI)	$\frac{1}{CN}$
Direction Selective Index (DSI)	$\frac{1}{\sqrt{\det\left((AA^T)^{\dagger}\right)}}$
Harmonic Mean Manipulability Index (HMMI)	$\operatorname{trace}\left(\left(AA^T\right)^{\dagger}\right)$
Stochastic Manipulability Index (SMI)	$\sqrt{nt} \times$ HMMI
Minimum Singular Value (MSV)	$\min\left(\sigma\left(AA^T\right)\right)$
Frobenius Norm (FN)	$\operatorname{trace}\left(\left(AA^T\right)^T\left(AA^T\right)\right)$

The Manipulability Index (MI) primarily quantifies the volume of the ellipsoid defined by Eq. (7). However, it solely represents magnitude and lacks information on

skewness of the ellipsoid. To address this limitation, the condition number (CN) is another candidate metric. However, since CN ranges from a minimum of 1 to infinity, it poses challenges in grasp analysis within the workspace. To mitigate this issue, the Local Condition Index (LCI) defined as the inverse of CN, provides a better sense of skewness and ranges from 0 to 1. The DSI offers a smoother transition near singularities by employing the pseudo-inverse. While an increase in one eigenvalue can inflate manipulability near singularity, it may not accurately reflect the grasp's quality. Hence, the HMMI utilizes the trace, capturing summation of eigenvalues' magnitudes. The SMI characterizes the hand's ability to move objects in various directions at different velocities, incorporating probability density functions. The MSV serves as a simple metric to assess a matrix's condition, offering insights into the grasp pose's proximity to singularity. Finally, the Frobenius Norm (FN) provides an indication of the matrix's size or magnitude, with a larger norm suggesting a matrix with more significant elements on average. We next discuss three simple and intuitive test cases to help compare the candidate metrics.

4 Test Cases for Manipulability Study

The three scenarios highlighted in this section encompass fundamental situations, including single-finger manipulation, two-dimensional grasp with two fingers, and three-dimensional grasp with four fingers. Below, we provide a detailed discussion of each case.

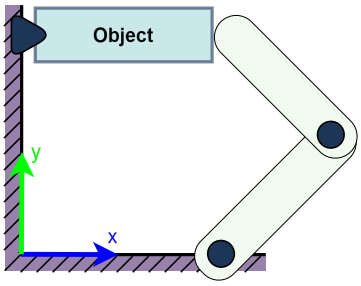


Fig. 2: One finger - HST

4.0.1 One-Finger Holding a Stick Task (HST)

Fig. 2 illustrates a schematic representation of a single finger holding the stick task. The object in this scenario is a stick that is held against a wall using a force applied by one finger on the other end of the stick. This scenario is modeled as a simplified scenario as the stick being pivoted at the wall via a revolute joint. Each link of the finger measures 3.5 cm in length, with the finger base positioned 14 cm from the wall. To analyze the indexes in the entire workspace of the finger, the length of the rod is varied from 7 cm to 21 cm. Various grasp indices are computed by rotating the rod by an angle $\phi \in [-\pi/2, \pi/2]$ about the point of contact with the wall.

4.0.2 Two-Finger HST

Similar to the one-finger analysis, we examine a scenario with two fingers (Fig. 3), each designed as an RR manipulator with equal link lengths. In line with the previous case, each link measures 3.5 cm in length, and the base spans 7 cm in width. The object's length matches that of the gripper base. The object is manipulated through various orientations ranging from $-\pi/2$ to $\pi/2$, and various y-axis positions.

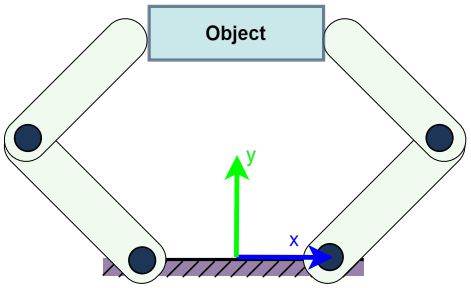


Fig. 3: Two-finger HST

4.0.3 Four-Finger Holding a Ball Task (HBT)

In this scenario as shown in Fig. 4, the gripper comprises a square base with dimensions of 7 cm, with fingers mounted on each corner. Each finger is modeled as an RRRR manipulator, featuring a base joint axis perpendicular to the axes of the subsequent three joints, enabling non-planar motion. The first link measures 1 cm in length, while the remaining links are 2 cm long. The spherical object of radius 1 cm is manipulated through various positions and orientation along the z-axis.

5 Analysis of Indexes

As detailed in Section 4, of the simulations conducted for all three cases, we first examine the variations in the values of different indices for the two-finger HST case as we vary object orientation and y position in Fig. 5. The value of the index is represented as a color map with the horizontal axis being the object orientation ϕ and vertical axis being the object vertical position coordinate y. Out of the 8 different indices, CN and FN do not provide sufficient information to analyze manipulability due to their mathematical formulations. Among the remaining 6 indices, two distinct trends emerge: MI, DSI, HMMI, and SMI exhibit similar trends, while LCI and MSV exhibit similar patterns. This observation holds true for the other two cases as well. Although magnitudes may vary, the trends remain consistent. Consequently, we conclude that MI and LCI are two crucial indices that capture different aspects of manipulability, encompassing both volume and skewness information. The remaining indices contribute redundant information along similar lines.

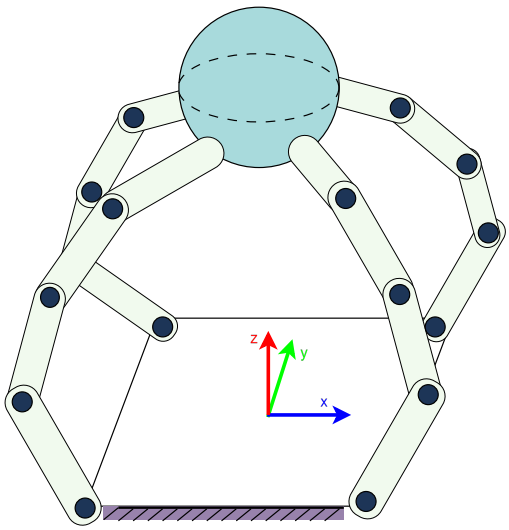


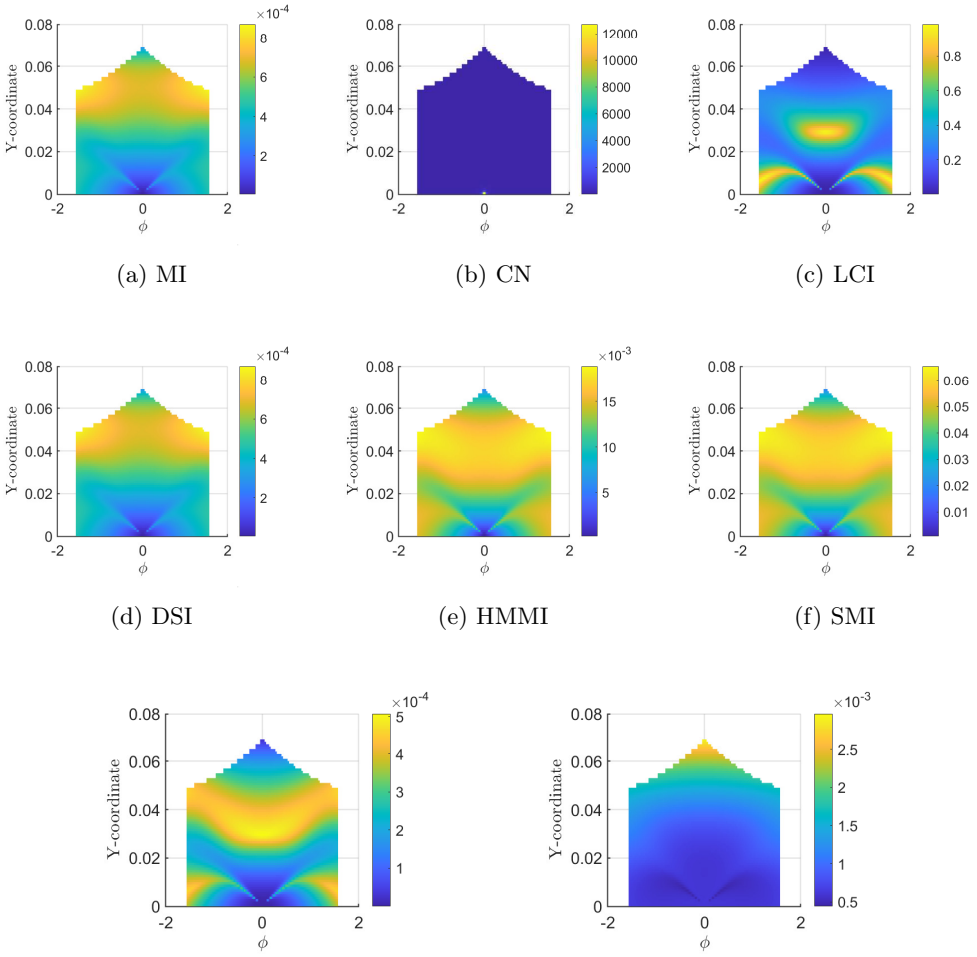
Fig. 4: Four-finger HBT

For MI, the highest values are observed when the object is rotated by small angles around the middle region of the workspace (Fig. 5a). At lower values of the y coordinate, higher manipulability is obtained when the object is oriented at larger angles, placing both manipulators near their respective high-manipulability regions. For extreme values of ϕ, the MI values remain moderately high when one of the two fingers is nearly fully extended, because the other finger still provides significant manipulation capability. The index values drop to zero only when both fingers simultaneously lose the ability to impart velocity in any direction.

LCI exhibits moderately high values in the middle region and in the high-orientation region when the object is close to the palm. This indicates that the corresponding grasp poses provide a more uniform ability to move the object in different directions. From Figs. 5a and 5c, it is evident that MI and LCI capture complementary information.

Both the MI and the LCI offer unique insights and drawbacks. While the former provides information about the volume of the ellipsoid, the latter offers insights into the variation in manipulability across different directions. Although the manipulability index may yield a high value, the matrix could be poorly conditioned. This discrepancy arises because manipulability inherently depends on the ellipse's volume, potentially resulting in a high volume for an elongated ellipse compared to a well-conditioned one.

Conversely, even when the matrix is well-conditioned, the ability to generate motion in any direction might be exceedingly low. Thus, it becomes necessary to mitigate these limitations to the greatest extent possible and develop a new index capable of capturing comprehensive information through a single metric, which not only captures important information corresponding to MI and LCI but also should be robust to change in the gripper design properties.



(a) MI (b) CN (c) LCI

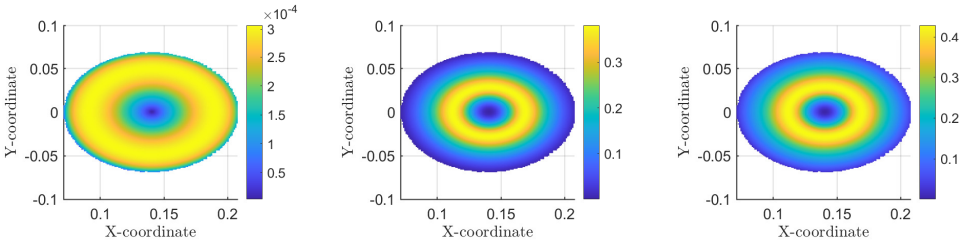
(d) DSI (e) HMMI (f) SMI

(g) MSV (h) FN

Fig. 5: The plots shown here display the properties of various indices for a two-RR-finger planar gripper for the HST. The stick is rotated about its centre of gravity, and the index values are plotted over the feasible finger workspace in Euclidean space. The condition number and Frobenius norm provide limited information for analysing grasp manipulability. Indices such as the local condition index and minimum singular value follow similar trends, while MI, DSI, HMMI, and SMI exhibit similar spatial patterns with differences in magnitude.

6 Grasp Dexterity Index

To address the limitations of the Manipulability Index (MI) and the Local Condition Index (LCI), we developed the Grasp Dexterity Index (GDI) as a hybrid metric that

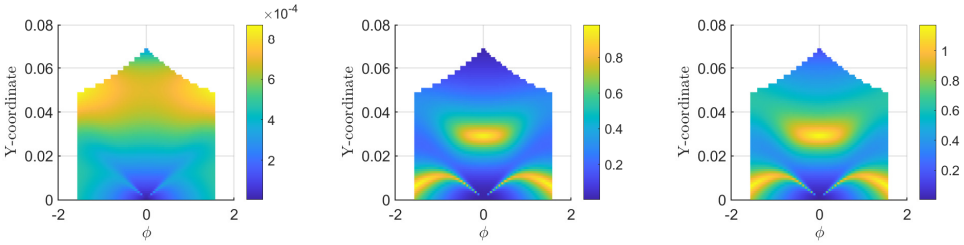


(a) MI (b) LCI (c) GDI

Fig. 6: Comparison of MI, LCI, and GDI for the one-finger HST. The stick is pivoted at the wall via a revolute joint, with its length varied from 7 cm to 21 cm and its orientation varied over $\phi \in [-\pi/2, \pi/2]$.

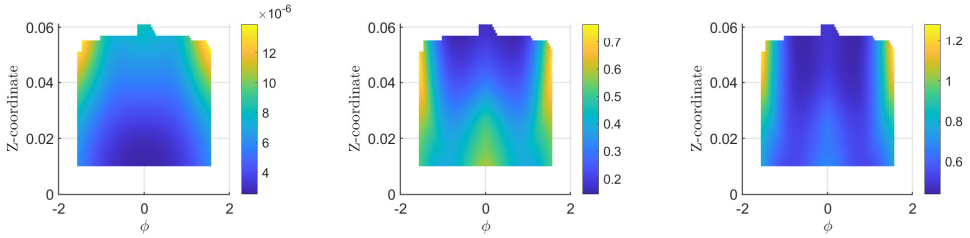
integrates the information of both MI and LCI. The GDI addresses a key challenge: reducing variations in index values caused by differences in gripper size and scaling. It achieves this by normalizing the MI using a characteristic length, which can be defined in various ways, such as the sum of all finger link lengths or the maximum link length. This normalization minimizes the impact of measurement unit differences and system scaling. In this work, we define the characteristic length as the maximum sum of the squares of link lengths across all fingers, ensuring consistent scaling and improved comparability across different robotic hand/graspers.

To integrate the updated MI and LCI, we considered both adding them together in different proportions and multiplying them together. Multiplying the indices together did not accurately capture their combined effect, as a low value in one metric resulted in an excessively low final metric. Conversely, adding the two metrics yielded more promising results, effectively representing their combined impact. We thus construct GDI as



(a) MI (b) LCI (c) GDI

Fig. 7: Comparison of MI, LCI, and GDI for the two-finger RR HST. Each finger is modeled as an RR manipulator with equal link lengths of 3.5 cm. The object length is equal to the gripper base width of 7 cm, and the object is manipulated over $\phi \in [-\pi/2, \pi/2]$ and different vertical positions.



(a) MI (b) LCI (c) GDI

Fig. 8: Comparison of MI, LCI, and GDI for the four-finger RRRR HBT. The gripper has a square base of 7 cm, with one finger mounted at each corner. Each finger is modeled as an RRRR manipulator, with a first link of 1 cm and remaining links of 2 cm. A spherical object of radius 1 cm is manipulated across different positions and orientations along the z-axis.

$$GDI \triangleq \lambda_1 \frac{MI}{max\left(\sum_{i=1}^{n_1} l_{1i}^m, \ldots, \sum_{i=1}^{n_k} l_{ki}^m\right)} + \lambda_2 LCI, \tag{8}$$

where m depends on whether the task space is 2-D ($m = 2$) or 3-D ($m = 3$), k denotes the number of contact points, and λ_1 and λ_2 are coefficients representing the relative weights of MI and LCI, with the condition that $\lambda_1 + \lambda_2 = 1$. Additionally, n_i indicates the number of links in the i^{th} finger.

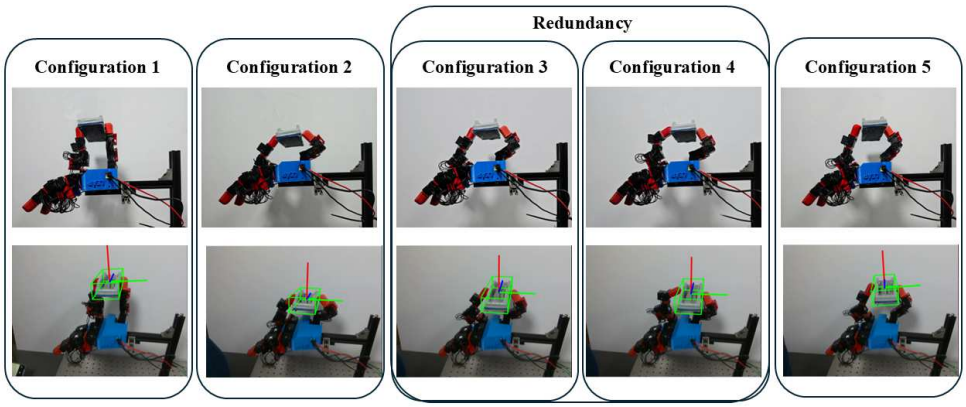
6.1 GDI for different test cases

Figs. 6, 7, and 8 present a comparison of MI, LCI, and GDI across all three test cases. Generally, the observed trends align well with the existing understanding of manipulability in serial chain manipulators. GDI tends to follow the patterns exhibited by the condition number, indicating a close relationship between the two metrics. By incorporating a scaled value of the MI, the GDI produces smoother surfaces, striking a balance between maximum manipulability and omnidirectional capability to impart velocities to the grasped object. Additionally, the values of the indices in each case fall within a similar range, suggesting that the grasp manipulability of grippers of similar sizes can potentially be compared using GDI values.

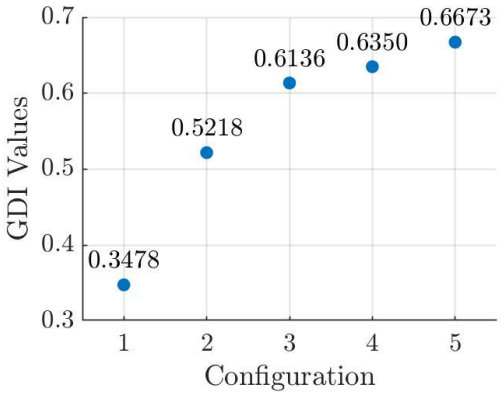
6.2 GDI for Redundancy Optimization

While the potential of GDI as a quantification of manipulability of the grasped object based on grasp configuration and in-hand positioning is obvious, we now turn our attention to redundant fingers with possible internal motions (without affecting grasp contact points and in-hand position of the object). To proceed, we first consider the two-finger HST case again but now with each finger being 3R instead of 2R (to incorporate redundancy) with the same total length of the fingers and dimensions of the

object. With this new redundant configuration, Fig. 10 showcases the values of GDI as a function of object y position and orientation ϕ. For this analysis, it is assumed that each finger has horizontal end effector orientation aligned with the palm and facing the object. Furthermore, to explore GDI's utility in optimizing over redundant config-



(a)



(b)

Fig. 9: Configurations of the LEAP Hand grasping a duster and the corresponding GDI values. (a) Five different grasp configurations are shown. Configurations 1 and 2 represent distinct poses with varied finger alignments. Configurations 3 and 4 are redundancy configurations, where the duster remains in the same position relative to the palm frame, but internal finger motions result in altered GDI values. Configuration 5 demonstrates another unique grasp pose. The bottom row highlights the corresponding object poses in bounding boxes obtained from the 6D pose estimation algorithm. (b) GDI values for the five configurations.

urations, for the same object position and orientation and we examine a range of last link angle from zero with respect to horizontal to negative 90 degrees to positive 90 degrees with respect to horizontal (thus representing internal motion without affecting contact points, object position or orientation). Fig. 11 illustrates the variation of GDI across this range of redundant configurations for a fixed object configuration. The object configuration corresponding to the maximum GDI value in Fig. 10 was selected for this analysis. This result shows that substantial variation in GDI can occur due to internal motion, with the possibility of multiple local maxima for a specific object configuration.

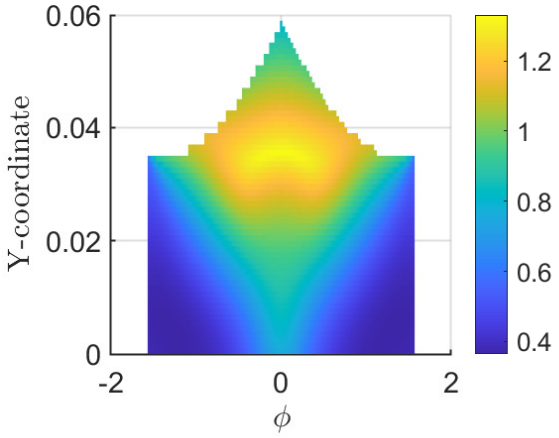


Fig. 10: GDI for 2-Finger HST with each finger being a RRR planar manipulator

7 Robot Grasping with GDI

In this section, we evaluate the Grasp Dexterity Index (GDI) in practical robotic setups to demonstrate its utility. The evaluation includes grasping and manipulation tasks performed using two distinct systems: the LEAP Hand and a bi-manual setup with two Franka Research Arms. The primary objective is to compute GDI values across various configurations and system scales, providing insights into how the index behaves under different conditions and highlighting its applicability in different robotic systems performing multi-arm coordination based manipulation.

7.1 Grasping with LEAP Hand

The LEAP Hand, developed by Carnegie Mellon University (CMU) [24], is a versatile robotic hand designed for advanced grasping and manipulation tasks. In this study, we utilize the LEAP Hand experimental setup to grasp a duster using a pinch grasp

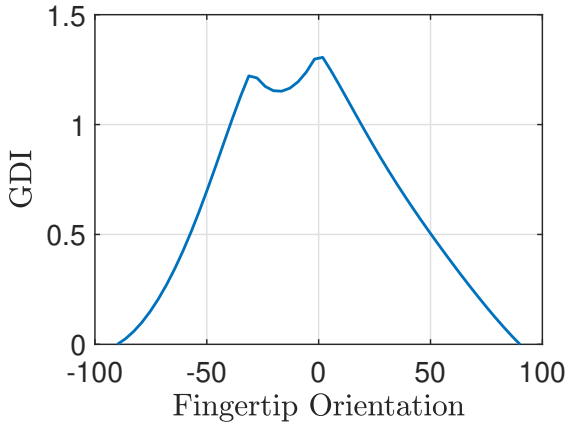
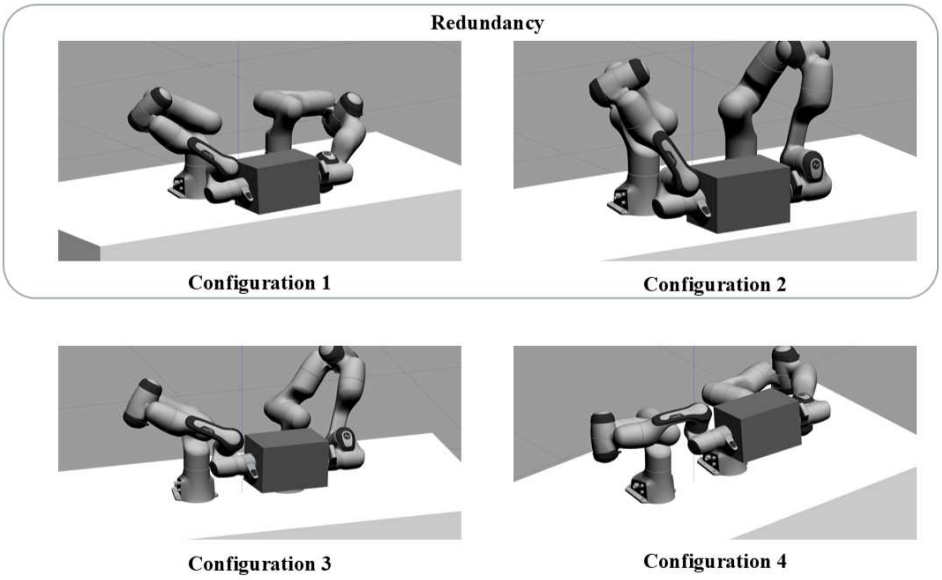


Fig. 11: GDI values of 50 redundant configurations for 2-Finger HST

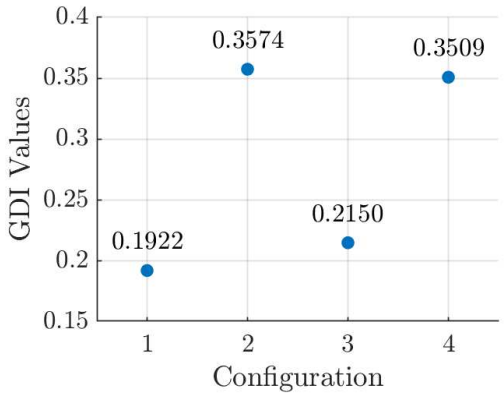
configuration, as illustrated in Fig. 9a. We evaluate the Grasp Dexterity Index (GDI) across five different configurations, shown in Fig. 9b. Among these, configurations 3 and 4 represent redundancy configurations where the duster's position relative to the palm remains unchanged, but variations in finger configurations due to internal motions result in differing GDI values. To compute the GDI, we first construct the grasp matrix, which requires the object's pose relative to the palm frame. For real-time tracking, we employed 6-D pose estimation, following the methodology outlined in [25]. Additionally, joint angles of the LEAP Hand were captured in real time to compute the hand Jacobian (J_H). Using this data, the GDI was calculated for each configuration. The results, depicted in Fig. 9a, reveal that the GDI is lowest when the fingers are fully extended, as observed in configuration 1, aligning with the theoretical understanding discussed in Section 5. For the pinch grasp of the duster, the GDI values range approximately between 0.3 and 0.7, demonstrating the index's sensitivity to finger configurations and grasp quality.

7.2 Bi-manual Manipulation with Two Franka Research 3 Arms

This section discusses a bi-manual manipulation task performed in simulation using Gazebo. The setup involves two 7-DOF Franka Research Arms tasked with picking up a box from a table and holding it in four different configurations along a direction perpendicular to the table. The Grasp Dexterity Index (GDI) was computed for each configuration, as shown in Fig. 12. Configurations 1 and 2 represent redundant configurations, where the box's position relative to the world frame remains unchanged, but internal arm motions lead to variations in GDI values. The GDI for these configurations lies in the range of 0.2–0.4, which is comparable to the values observed in the LEAP Hand task. Despite the significant differences in the size and scale of the two systems, the results highlight the GDI's ability to provide a comparable measure of manipulability across diverse robotic systems.

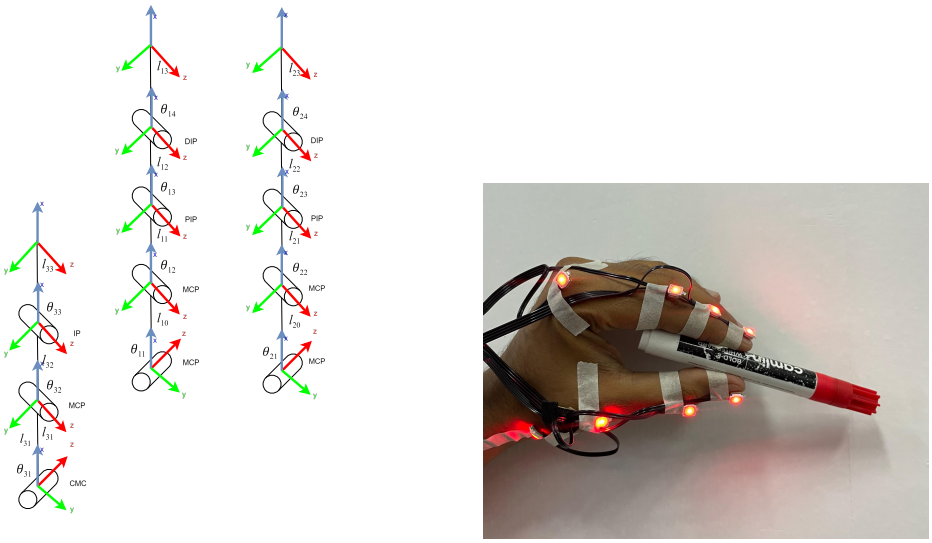


(a)



(b)

Fig. 12: Bi-manual manipulation configurations in simulation and the corresponding GDI values. (a) Four configurations of a bi-manual task using two 7-DOF Franka Research Arms in Gazebo are shown. Configurations 1 and 2 are redundancy configurations with the box in the same position but different internal arm motions. Configurations 3 and 4 depict distinct arm poses manipulating the box. (b) GDI values for the four configurations.



(a) (b)

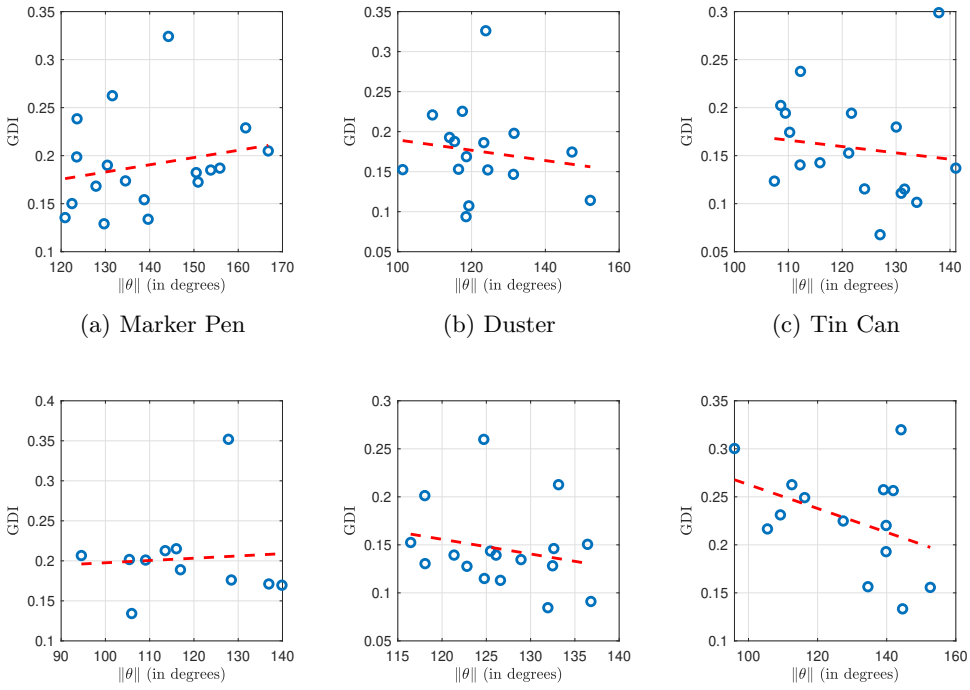
Fig. 13: (a) Human hand kinematic representation: From left to right, thumb, index finger, and middle finger. and (b)Human hand grasping a marker for dexterity analysis: A human hand with motion tracking sensors grasping a marker in a pinch grasp configuration, used to evaluate grasp dexterity and monitor finger positions.

8 Human Grasping

Since humans are renowned for their remarkable dexterity, we next apply GDI to a human grasp pilot study. In our daily activities, we frequently employ grasps that fall within the pinch and tripod categories, as outlined in the grasp taxonomy [26]. These grips, with soft point contacts, are among the most commonly utilized precision grasp poses for object manipulation. Given the impressive capabilities of humans in this regard, our objective was to conduct a pilot study with human subjects to investigate how GDI correlates with human grasp patterns.

8.1 Hand Modeling

In our study, for simplicity, we employed a rigid kinematic model for the thumb, index finger, and middle finger [27]. For this paper, the thumb model has been further simplified. As illustrated in Fig. 13a, flexion-extension and internal rotation of the carpometacarpal (CMC) joint are included as part of the palm frame, while adduction-abduction of the metacarpophalangeal (MCP) joint is excluded, as the thumb was observed to have minimal effect on the tripod and pinch grasp strategies. For the index and middle fingers (Fig. 13a), all motions are considered to model the grasp accurately. Finger twists are neglected, and the finger segments are considered rigid.



(a) Marker Pen (b) Duster (c) Tin Can

(d) Geometry Box (e) TT Ball (f) Disc

Fig. 14: GDI values versus joint-angle norm for tripod grasp across six objects.

As detailed in Fig. 13a, the base frame of the index and middle finger is situated at its MCP joint and the base frame of the thumb is located at its CMC joint, with the base frame of the index finger also serving as the palm frame. Let l_{31}, l_{32}, and l_{33} represent the link lengths of the thumb; l_{11}, l_{12}, and l_{13} denote the link lengths of the index finger; and l_{21}, l_{22}, and l_{23} refer to the link lengths of the middle finger. Similarly, θ_{31}, θ_{32}, and θ_{33} signify the adduction-abduction of the MCP joint, flexion-extension of the CMC joint, and flexion-extension of the interphalangeal joint (IP) of the thumb, respectively. For the index finger, θ_{11}, θ_{12}, θ_{13}, and θ_{14} correspond to the adduction-abduction of the MCP joint, flexion-extension of the MCP joint, flexion-extension of the proximal interphalangeal (PIP) joint, and flexion-extension of the distal interphalangeal (DIP) joint, respectively. The middle finger joints, θ_{21}, θ_{22}, θ_{23}, and θ_{24}, are defined similarly to those of the index finger. A frictional point contact model was utilized for the experiment, and Denavit-Hartenberg (D-H) parameters were formulated to derive the Jacobian matrix for each finger.

8.2 Experimental Methodology

Twenty-one young, healthy, right-handed subjects (19 males and 2 females) participated in the human grasp experiment. The experiment was approved by the Institute

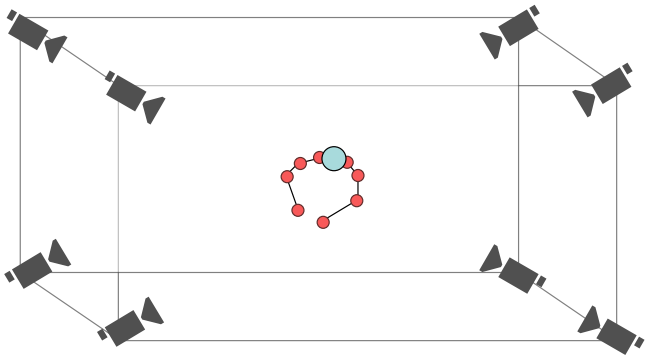


Fig. 15: Representative diagram of Motion Capture System

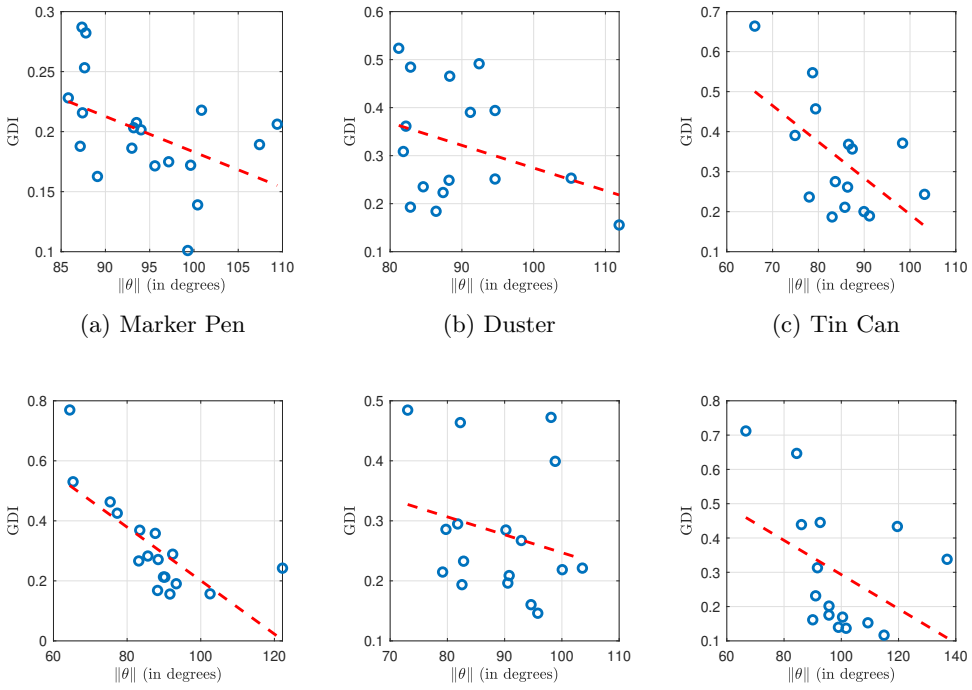
Ethics Committee at the Indian Institute of Technology Gandhinagar. Subjects were asked to grasp six lightweight objects (marker pen, geometry box, duster, tin can, table tennis ball, and flat disc) to study human grasping behavior. The PhaseSpace motion capture system was utilized to monitor finger movements, with LED markers mounted on the IP, DIP, PIP, MCP, and CMC joints. Eight cameras were positioned at the corners of a cuboidal frame. A representative diagram for experimental data collection is shown in Fig. 15.

The LED markers were secured using Velcro straps and medical-grade tapes, and additional markers were attached to the objects to capture their configuration in 3D space (Fig. 15). The objects were lightweight and rigid to minimize the effects of gravity and contact mechanics. Participants were given time to familiarize themselves with the objects before the trials. They were instructed to use their fingertips to grasp the objects in a manner that allowed for maximum movement without losing contact. Subjects performed two types of grasps: pinch (using the thumb and index finger) and tripod (using the thumb, index finger, and middle finger). Marker positions were recorded at 960 Hz throughout the experiments.

8.3 Analysis

The experimental data was processed using MATLAB. The motion capture data was averaged over 20 samples and accordingly down sampled. Joint angles and coordinate frames were derived from the LED marker data. GDI was computed for each trial and plotted against the norm of the finger joint angles. From Figs. 16 and 14, it can be clearly observed that GDI enriches the characterization of grasp types based on finger joint angles. Over the limited range of angle norms observed, GDI appears to be negatively correlated with norm of angle in most cases. Similarly, GDI varies with the norm of finger lengths (not presented here for brevity). Furthermore, GDI incorporates gripper/hand parameters to assess the feasibility and quality of the grasp.

Overall, GDI showed a higher correlation with the norm of joint angles for the tripod grasp, while finger lengths demonstrated a higher correlation in the pinch grasp. As observed in Fig. 17, GDI for tripod grasp has less variation across subjects for all the objects when compared to the pinch grasp. Moreover, the pinch grasp has



(a) Marker Pen (b) Duster (c) Tin Can

(d) Geometry Box (e) TT Ball (f) Disc

Fig. 16: GDI values versus joint-angle norm for pinch grasp across six objects.

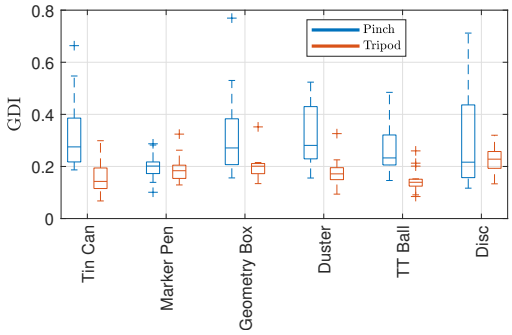


Fig. 17: Tripod and Pinch grasp boxplot

higher GDI values than the tripod grasp. This appears to indicate that pinch grasp in general affords higher manipulability than tripod grasp and is intuitively obvious. Additionally, the experiment confirms the effectiveness of the scaling factor for manipulability, as GDI values lie within a similar range and can be used to compare the grasp manipulability of grippers/hands of different sizes.

This experiment serves as a pilot study, laying the groundwork for further research. Future work can explore in-hand manipulation planning by maximizing the grasp manipulability index for specific tasks.

9 Conclusion

With an increasing interest in multi-finger, multi-DOF robot hands for manipulating grasped objects, there is a need for a simple and practical metric for evaluating grasp manipulability. We proposed a new metric, Grasp Dexterity Index (GDI) that incorporates elements of manipulability and ability to move the objects in all directions. Using this metric, we examined three test scenarios and the effect of in-hand positioning and internal (redundant) motion of fingers on grasp manipulability. Further, using a pilot-scale human study with six day-to-day objects, we demonstrated the utility of GDI. GDI was able to predict configurations for best manipulability in the test simulations scenarios and was able to help different manipulability capabilities in pinch grasp and tripod grasp in the human subject studies.

10 Future Work

GDI is a promising first step toward formulating a practical and simple metric for assessing grasp manipulability. However, there is scope for further exploration and improvement. GDI currently does not account for the ability to impart angular velocities to the grasped object, as the entire framework only considers the translational component of grasping functions. Additionally, this framework does not include the effects of soft contact points. Furthermore, exploring more robust normalization methods for the Manipulability Index (MI) could ensure the GDI is fully scale- and unit-invariant, making it applicable across diverse robotic systems and configurations.

Future work could adopt a power-based approach to combine the capabilities of generating both angular and translational velocities in the object. Further development is also needed to create an index that evaluates the force application ability for a given grasp. A combined understanding of force and velocity generation in grasping applications will establish a strong foundation for exploring the field of precision grasp planning.

Acknowledgements. The authors are thankful to Mr. Rajesh Kumar, Mr. Ashutosh Goyal, and Mr. Ravi Dhoria for their help with the simulations. The authors gratefully acknowledge support in part from the Science and Engineering Research Board through grant number CRG/2022/005196, and from the Gujarat Council on Science and Technology through grant number GUJCOST/STI/2023-24/338. The first author also acknowledges support from the Prime Minister's Research Fellowship (PMRF) scheme (ID No. 1702149). Finally, the authors thank IIT Gandhinagar for their continued support.

Declarations

Funding. The authors gratefully acknowledge support in part from the Science and Engineering Research Board through grant number CRG/2022/005196, and from the Gujarat Council on Science and Technology through grant number GUJCOST/STI/2023-24/338. The first author also acknowledges support from the Prime Minister's Research Fellowship (PMRF) scheme (ID No. 1702149).

Conflict of interest. The authors declare that they have no competing interests.

Ethics approval and consent to participate. The human grasping experiment was approved by the Institute Ethics Committee at the Indian Institute of Technology Gandhinagar. Informed consent was obtained from all participants prior to participation in the study.

Consent for publication. Not applicable.

Data availability. The datasets generated and analyzed during the current study are available from the corresponding author on reasonable request.

Code availability. The code used for the analysis is available from the corresponding author on reasonable request.

Author contribution. S. Barat and Vatsal Ketankumar Joshi contributed equally to this work. S. Barat and Vatsal Ketankumar Joshi contributed to the primary conceptualization of the study, methodology development, simulation design, analysis of results, and initial manuscript preparation. Debojit Das contributed to the Gazebo-based bi-manual simulation study, manuscript writing, editing, formatting, and technical discussions. Harish J. Palanthandalam-Madapusi supervised the study, provided technical guidance, contributed to the interpretation of results, and reviewed and edited the manuscript. All authors reviewed and approved the final manuscript.

References

[1] Bohg, J., Morales, A., Asfour, T., Kragic, D.: Data-driven grasp synthesis—a survey. IEEE Transactions on Robotics **30**(2), 289–309 (2014) https://doi.org/10.1109/TRO.2013.2289018

[2] Shimoga, K.B.: Robot grasp synthesis algorithms: A survey. The International Journal of Robotics Research **15**(3), 230–266 (1996)

[3] Rimon, E., Burdick, J.: The Kinematics and Mechanics of Grasping Mechanisms, pp. 411–436. Cambridge University Press, Cambridge, United Kingdom (2019)

[4] Borst, C., Fischer, M., Hirzinger, G.: Grasp planning: how to choose a suitable task wrench space. In: IEEE International Conference on Robotics and Automation, 2004. Proceedings. ICRA '04. 2004, vol. 1, pp. 319–3251 (2004). https://doi.org/10.1109/ROBOT.2004.1307170

[5] Tan, T., Alqasemi, R., Dubey, R., Sarkar, S.: Formulation and validation of an intuitive quality measure for antipodal grasp pose evaluation. IEEE Robotics and Automation Letters **6**(4), 6907–6914 (2021) https://doi.org/10.1109/LRA.2021.3096192

[6] Roa, M.A., Suárez, R.: Grasp quality measures: review and performance. Autonomous robots **38**, 65–88 (2015)

[7] Xu, R., Luo, J., Wang, M.: Optimal grasping pose for dual-arm space robot cooperative manipulation based on global manipulability. Acta Astronautica **183**, 300–309 (2021) https://doi.org/10.1016/j.actaastro.2021.03.021

[8] Xu, R., Luo, J., Wang, M.: Kinematic and dynamic manipulability analysis for free-floating space robots with closed chain constraints. Robotics and Autonomous Systems **130**, 103548 (2020) https://doi.org/10.1016/j.robot.2020.103548

[9] Prattichizzo, D., Malvezzi, M., Gabiccini, M., Bicchi, A.: On the manipulability ellipsoids of underactuated robotic hands with compliance. Robotics and Autonomous Systems **60**(3), 337–346 (2012) https://doi.org/10.1016/j.robot.2011.07.014 . Autonomous Grasping

[10] Li, J., Ganguly, A., Figueredo, L.F., Haddadin, S.: The fingertip manipulability assessment of tendon-driven multi-fingered hands. IEEE Robotics and Automation Letters (2024)

[11] Kumar, R., Mukherjee, S.: Algorithmic Selection of Preferred Grasp Poses Using Manipulability Ellipsoid Forms. Journal of Mechanisms and Robotics **14**(5), 051006 (2022) https://doi.org/10.1115/1.4053374

[12] Cheng, H., Wang, Y., Meng, M.Q.-H.: A robot grasping system with single-stage anchor-free deep grasp detector. IEEE Transactions on Instrumentation and Measurement **71**, 1–12 (2022) https://doi.org/10.1109/TIM.2022.3165825

[13] Weng, T., Held, D., Meier, F., Mukadam, M.: Neural Grasp Distance Fields for Robot Manipulation (2023). https://arxiv.org/abs/2211.02647

[14] Goins, A.K., Carpenter, R., Wong, W.-K., Balasubramanian, R.: Implementation of a gaussian process-based machine learning grasp predictor. Autonomous Robots **40**, 687–699 (2016)

[15] Wei, J., Liu, H., Yan, G., Sun, F.: Robotic grasping recognition using multi-modal deep extreme learning machine. Multidimensional Systems and Signal Processing **28**, 817–833 (2017)

[16] Shang, W., Song, F., Zhao, Z., Gao, H., Cong, S., Li, Z.: Deep learning method for grasping novel objects using dexterous hands. IEEE Transactions on Cybernetics

52(5), 2750–2762 (2022) https://doi.org/10.1109/TCYB.2020.3022175

[17] Wang, L., Xiang, Y., Yang, W., Mousavian, A., Fox, D.: Goal-Auxiliary Actor-Critic for 6D Robotic Grasping with Point Clouds (2021). https://arxiv.org/abs/2010.00824

[18] Calandra, R., Owens, A., Jayaraman, D., Lin, J., Yuan, W., Malik, J., Adelson, E.H., Levine, S.: More than a feeling: Learning to grasp and regrasp using vision and touch. IEEE Robotics and Automation Letters **3**(4), 3300–3307 (2018) https://doi.org/10.1109/lra.2018.2852779

[19] Geng, T., Lee, M., Hülse, M.: Transferring human grasping synergies to a robot. Mechatronics **21**(1), 272–284 (2011) https://doi.org/10.1016/j.mechatronics.2010.11.003

[20] Feix, T., Romero, J., Ek, C.H., Schmiedmayer, H.-B., Kragic, D.: A metric for comparing the anthropomorphic motion capability of artificial hands. IEEE Transactions on Robotics **29**(1), 82–93 (2013) https://doi.org/10.1109/TRO.2012.2217675

[21] Liu, C., Fang, B., Sun, F., Li, X., Huang, W.: Learning to grasp familiar objects based on experience and objects' shape affordance. IEEE Transactions on Systems, Man, and Cybernetics: Systems **49**(12), 2710–2723 (2019) https://doi.org/10.1109/TSMC.2019.2901955

[22] Nakajima, T., Asami, Y., Endo, Y., Tada, M., Ogihara, N.: Prediction of anatomically and biomechanically feasible precision grip posture of the human hand based on minimization of muscle effort. Scientific Reports **12**(1), 13247 (2022)

[23] Patel, S., Sobh, T.: Manipulator performance measures-a comprehensive literature survey. Journal of Intelligent & Robotic Systems **77**, 547–570 (2015)

[24] Shaw, K., Agarwal, A., Pathak, D.: Leap hand: Low-cost, efficient, and anthropomorphic hand for robot learning. arXiv preprint arXiv:2309.06440 (2023)

[25] Wen, B., Yang, W., Kautz, J., Birchfield, S.: Foundationpose: Unified 6d pose estimation and tracking of novel objects. In: Proceedings of the IEEE/CVF Conference on Computer Vision and Pattern Recognition, pp. 17868–17879 (2024)

[26] Feix, T., Romero, J., Schmiedmayer, H.-B., Dollar, A.M., Kragic, D.: The grasp taxonomy of human grasp types. IEEE Transactions on Human-Machine Systems **46**(1), 66–77 (2016) https://doi.org/10.1109/THMS.2015.2470657

[27] Lenarčič, J., Bajd, T., Stanišić, M.M.: Kinematic Model of the Human Hand, pp. 313–326. Springer, Dordrecht (2013)